Review Article

Noureddine Kheloufi* and Abdellatif Dehni

Some mathematical assumptions for accurate transformation parameters between WGS84 and Nord Sahara geodetic systems

https://doi.org/10.1515/jogs-2022-0160 received June 20, 2022; accepted October 31, 2023

Abstract: The transformation of coordinates between different geodetic datums has been a common practice within the geospatial profession. Relating different geodetic datums mostly involves the use of conformal transformation techniques, which could produce results that are not very often satisfactory for certain geodetic, surveying, and mapping purposes. This has been attributed to the inability of the conformal models to resolve the lack (non-exhaustivity) and the heterogeneity of double points existing within the Algerian local geodetic networks. Indeed, the Algerian geodetic network is divided into two main zones completely different in accuracy and points exhaustivity. The North is better and well defined in precision; on the other hand, the South is poorly defined because of the lack of heterogeneity of the points. Mathematical algebraic methods give closed-form solutions to geodetic transformation problems, requiring a high-level computer programming background. In everyday usage, the closed-form solutions are much simpler and have a higher precision than earlier procedures. Thus, it can be predicted that these new solutions will find their place in practice. The present work deals with an important theoretical problem of geodesy: we are looking for a mathematical dependency between two spatial systems using common pairs of points whose coordinates are given in both systems. In geodesy and photogrammetry, the most often used procedure to move from one coordinate system to another is the 3D, seven-parameter similarity transformation (Bursa-Wolf, Molodensky-Badekas, and Helmert).

Keywords: Bursa–Wolf, Helmert, spatial coordinates, similarity, transformation

1 Introduction

3D conformal transformations, also known as similarity transformations (since conformal transformations preserve shape and angles between vectors in space remain unchanged), are commonly used in surveying, photogrammetry, and geodesy. These transformations are necessary for the purposes of cartography, geodesy, and other topographical and cadastral work when the coordinates are generally expressed in the system in effect in a country. The present work consists of developing a strategy of observation, processing double geodetic networks with a view to the comparison between the different transformation models (Bursa-Wolf, Molodensky-Badekas, 2D-multiple regression, etc.), and the realization of a geographical coordinates planimetric conversion grid between the WGS84 system and other national systems like the Algerian North Sahara Datum (Kheloufi et al., 2009).

3D transformations are usually applied to convert coordinates related to one geodetic datum to another; this operation is commonly known as a datum transformation. In such applications, the rotations between the two 3D coordinate axes are small (usually less than 1s of arc), and certain approximations are used to simplify rotation matrices; these simplified matrices are a common feature of the Bursa–Wolf and the Molodensky–Badekas transformations.

The transformation of GPS data into the geodetic local system, which is the basis of the mapping system in force in every country and in which the results of geodetic work must be expressed, requires knowledge of the passage parameters with the use of a suitable model. The choice of transformation model requires the availability of a dataset known in each of the two systems.

The transformation is presented either in similarity form nor under geographic formalism known as the

^{*} Corresponding author: Noureddine Kheloufi, Department of Spatial Geodesy, Centre of Space Techniques (CTS), Agence Spatiale Algerienne (ASAL), Arzew, Algeria, e-mail: nkheloufi@cts.asal.dz, tel: +213-41-79-30-42 Abdellatif Dehni: Department of SIRS, Centre of Space Techniques (CTS), Agence Spatiale Algerienne (ASAL), Arzew, Algeria, e-mail: adehni@cts.asal.dz

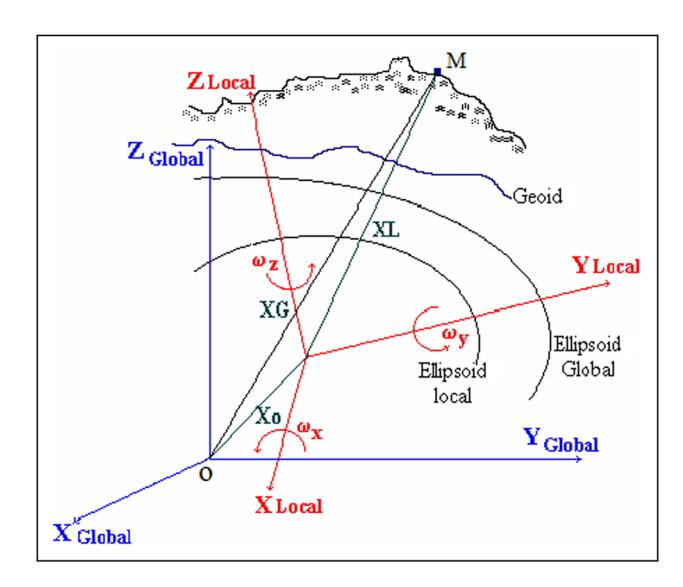


Figure 1: Translations and rotations between two systems.

Molodensky model (Figure 1) or a bi-dimensional 2D affine regression.

1.1 General shape of geodetic transformation

Let I, I, K be the orthogonal base of system O, X, Y, Z and i, j, k be that of system O, x, y, z.

We have
$$\overrightarrow{OM} = X \cdot \overrightarrow{I} + Y \cdot \overrightarrow{J} + Z \cdot \overrightarrow{K}$$
 in (O, X, Y, Z) .
 $\overrightarrow{OM} = x \cdot \overrightarrow{i} + y \cdot \overrightarrow{j} + z \cdot \overrightarrow{k}$ in (O, x, y, z) .

The vector \overrightarrow{OM} has X, Y, and Z as components, which are the orthogonal projections on OX, OY, and OZ.

$$X = O\vec{M} \cdot \vec{I} = (x \cdot \vec{i} + y \cdot \vec{j} + z \cdot \vec{k}) \cdot \vec{I}$$

$$Y = O\vec{M} \cdot \vec{J} = (x \cdot \vec{i} + y \cdot \vec{j} + z \cdot \vec{k}) \cdot \vec{J}$$

$$Z = O\vec{M} \cdot \vec{K} = (x \cdot \vec{i} + y \cdot \vec{j} + z \cdot \vec{k}) \cdot \vec{K}.$$
(1)

Hence,

$$\begin{pmatrix} X \\ Y \\ Z \end{pmatrix} = \begin{pmatrix} \vec{i} \cdot \vec{I} & \vec{j} \cdot \vec{I} & \vec{k} \cdot \vec{I} \\ \vec{i} \cdot \vec{J} & \vec{j} \cdot \vec{J} & \vec{k} \cdot \vec{J} \\ \vec{i} \cdot \vec{K} & \vec{j} \cdot \vec{K} & \vec{k} \cdot \vec{K} \end{pmatrix} \cdot \begin{pmatrix} x \\ y \\ z \end{pmatrix}.$$
 (2)

2 Earlier development of transformation formalisms

The names of the two transformations are an acknowledgment to the authors Bursa (1962), Wolf (1963), Molodensky et al. (1960), and Badekas (1969) of technical papers and reports on transformation methods related to the orientation of reference ellipsoids and 3D geodetic networks. 3D conformal transformations for single points are often given in the vectorial form (Collilieux et al., 2016).

The two most commonly used 3D models (Molodensky and Bursa) have the following global simplified formalism:

Molodensky-Badekas:

$$\vec{X} = \vec{X}_0 + \vec{T} + (1 + \Delta k) \cdot (I + \Delta R) \cdot (\vec{X} - \vec{X}_0), \tag{3}$$

Bursa-Wolf:

$$\vec{X} = \vec{T} + (1 + \Delta k) \cdot (I + \Delta R) \cdot \vec{X}. \tag{4}$$

where \vec{X} is the coordinate vector in the target system. \vec{X} is the coordinate vector in the origin system, \vec{x}_0 is the coordinate vector of barycenter in the origin system, \overrightarrow{T} is the translation vector, ΔR is the variation of the two systems rotation, I is the identity matrix, and Δk is the scale factor variation between metrics of the two systems, generally equal to zero, except in the case of projection from spherical curved coordinates to planar topographical surface.

The mathematical relationship can be written in such a way as to be able to consider the transformation parameters as unknown and thus be able to estimate them. Such a form is that we can estimate the transformation parameters knowing the coordinates in both systems by the following equation (Boateng, 2016):

$$\begin{bmatrix} X \\ Y \\ Z \end{bmatrix} = \begin{bmatrix} x \\ y \\ z \end{bmatrix} + \begin{bmatrix} 1 & 0 & 0 & x & 0 & z & -y \\ 0 & 1 & 0 & y & -z & 0 & x \\ 0 & 0 & 1 & z & y & -x & 0 \end{bmatrix} . \begin{bmatrix} Tx \\ Ty \\ Tz \\ dk \\ Ex \\ Ey \\ Ez \end{bmatrix}$$
 (5)

These two equations could not be obtained without supposing some assumptions for a geodetic mathematical hypothesis in order to lead to these canonical linear formalisms (equation (7)).

In the Molodensky formalism Molodensky (1960), the computation of transformation parameters goes in general through the barycenter coordinates written in both systems (Kheloufi, 2012):

$$\vec{X}_{0} \begin{pmatrix} X_{0} \\ Y_{0} \\ Z_{0} \end{pmatrix} = \begin{bmatrix} \frac{\sum_{i=1}^{n} X_{i}}{n} \\ \frac{\sum_{i=1}^{n} Y_{i}}{n} \\ \frac{\sum_{i=1}^{n} Z_{i}}{n} \end{bmatrix}, \quad \vec{X}_{0} \begin{pmatrix} X_{0} \\ Y_{0} \\ Z_{0} \end{pmatrix} = \begin{bmatrix} \frac{\sum_{i=1}^{n} X_{i}}{n} \\ \frac{\sum_{i=1}^{n} Y_{i}}{n} \\ \frac{\sum_{i=1}^{n} Z_{i}}{n} \end{bmatrix}.$$

$$Systemn^{\circ} 1 \qquad Systemn^{\circ} 2$$

$$(6)$$

As a result, in matricial form, the Molodensky formalism for a set of *n*-points is as follows:

$$\begin{pmatrix}
X_{1} - x_{1} \\
X_{2} - x_{2} \\
... \\
X_{n} - x_{n} \\
Y_{1} - y_{1} \\
Y_{2} - y_{2} \\
... \\
Y_{n} - y_{n} \\
Z_{1} - z_{1} \\
Z_{2} - z_{2} \\
... \\
Z_{n} - z_{n}
\end{pmatrix} = \begin{pmatrix}
1 & 0 & 0 & \bar{x}_{1} & 0 & \bar{z}_{1} & -\bar{y}_{1} \\
1 & 0 & 0 & \bar{x}_{2} & 0 & \bar{z}_{2} & -\bar{y}_{2} \\
... & ... & ... & ... \\
1 & 0 & 0 & \bar{x}_{n} & 0 & \bar{z}_{n} & -\bar{y}_{n} \\
0 & 1 & 0 & \bar{y}_{1} - \bar{z}_{1} & 0 & \bar{x}_{1} \\
0 & 1 & 0 & \bar{y}_{2} - \bar{z}_{2} & 0 & \bar{x}_{2} \\
... & ... & ... & ... & ... \\
0 & 1 & 0 & \bar{y}_{n} - \bar{z}_{n} & 0 & \bar{x}_{n} \\
0 & 0 & 1 & \bar{z}_{1} & \bar{y}_{1} & -\bar{x}_{1} & 0 \\
0 & 0 & 1 & \bar{z}_{2} & \bar{y}_{2} & -\bar{x}_{2} & 0 \\
... & ... & ... & ... & ... \\
0 & 0 & 1 & \bar{z}_{n} & \bar{y}_{n} & -\bar{x}_{n} & 0
\end{pmatrix} \cdot \begin{pmatrix} Tx \\ Ty \\ Tz \\ Ak \\ Ex \\ Ey \\ Ez \end{pmatrix}$$
where \bar{x}_{1} , \bar{x}_{2} and \bar{z}_{1} are the coordinates of the isobarycen-

where \bar{x}_i , \bar{y}_i , and \bar{z}_i are the coordinates of the isobarycenters in both systems (Novikova, 2020). This model (Molodensky-Badekas) is known as a Cartesian formalism and is obtained by the introduction of a vector and an initial point x_0 around which (E_x, E_y, E_z) rotations are performed. This point is generally considered an isobarycenter in both coordinate systems Collier (2020). This model is often used for local, wide-scale transformations (land survey, civil engineering, etc.; equation (7)).

3 Some problems in Molodensky-Badekas and **Bursa-Wolf transformations**

In reality, the Molodensky transformation is described as shown in Figure 2, where the centroid G is displaced from O2 by translations t_X , t_Y , and t_Z measured in the directions of the X, Y, and Z axes of system 2 and $t_2 = [t_X \ t_Y \ t_Z]_2^T$ is the position of the vector of the centroid. The mathematical relationship between the two systems via this transformation is, in reality, more complex than its final known form and is written as follows (Zavoti and Kalmár, 2016):

$$\overline{I}_{1} = \begin{bmatrix} \overline{X} \\ \overline{Y} \\ \overline{Z} \end{bmatrix}_{1} = \begin{bmatrix} X - X_{G} \\ Y - Y_{G} \\ Z - Z_{G} \end{bmatrix} = I_{1} - g_{1}. \tag{8}$$

The Figure 2 illustrates graphically the complexity and differences in the implementation of the two 3D transformations relevant to the type of data (point coordinates) and the expected accuracy as a function of the purpose of the transformation.

3.1 Adopted assumptions

Because the mathematical formalism differs in substance and the geodetic network is not of the same type and size (order 0-4), some assumptions are mandatory for an accurate estimation of transformation parameters using either 3D or 2D models Helmert (1907), as shown below.

3.1.1 First assumption

By identifying the scalar products in a real nonlinear rotation matrix, we obtain

$$\vec{i} \cdot \vec{I} = \cos E_y \cdot \cos E_z$$

$$\vec{j} \cdot \vec{I} = \cos E_z \cdot \sin E_y \cdot \sin E_x - \sin E_z \cdot \cos E_x$$

$$\vec{k} \cdot \vec{I} = \sin E_z \cdot \sin E_x + \cos E_z \cdot \sin E_y \cdot \cos E_x$$

$$\vec{i} \cdot \vec{J} = \sin E_z \cdot \cos E_y$$

$$\vec{j} \cdot \vec{J} = \cos E_z \cdot \cos E_x + \sin E_z \cdot \sin E_y \cdot \sin E_x$$

$$\vec{k} \cdot \vec{J} = -\cos E_z \cdot \sin E_x + \sin E_z \cdot \sin E_y \cdot \cos E_x$$

$$\vec{i} \cdot \vec{K} = -\sin E_y$$

$$\vec{j} \cdot \vec{K} = \cos E_y \cdot \sin E_x$$

$$\vec{k} \cdot \vec{K} = \cos E_x \cdot \cos E_y$$

where E_x , E_y , and E_z are rotations around the three axes OX, OY, and OZ, respectively.

In this study, the third coordinate, the orthometric height, would be assimilated as an ellipsoidal height, provided by satellite observation in the global navigation satellites systems (GNSS) survey (Marcin, 2011). This assimilation blemished the results considerably, but the assumptions made in this article have compensated for the lack of data and corrected them (Ziggah et al., 2017).

In addition, the double point coordinates have been attached to the last version of the terrestrial reference frame built on the base of GNSS permanent stations. These stations are dispatched all over the world, and their coordinates are determined by considering crustal deformations and geodynamics and processed by time series (Kheloufi, 2012).

Case in geodesy

Due to the construction of any two geodetic reference systems are close to each other and the orders of magnitude of the rotation angles are relatively small.

The parameters involved in a transformation are summarized as follows:

- The translations T_x , T_y , and T_z are less than a few hundred meters.
- The rotations E_x , E_y , and E_z are of the order of a few seconds of arc.

For small rotation angles, the rotation matrix may be simplified by the approximations:

 $\cos \varepsilon_x \approx 1$ $\sin \varepsilon_x \approx \varepsilon_x \text{ (rad)}$ $\sin \varepsilon_z, \sin \varepsilon_v \approx 0$

From equations (4) and (5), we obtain the simple linear form of the rotation matrix as in equation (9).

• The scale factor is close to unity; we can write that $K = 1 + \delta k$ and that $\delta k < 0.000001$.

The matrix became skew-symmetric and led us to conclude that this rotation matrix $R(E_x, E_z, E_y)$ can be "linearized" as follows:

$$R = \begin{pmatrix} 1 & -E_z & E_y \\ E_z & 1 & -E_x \\ -E_y & E_x & 1 \end{pmatrix}. \tag{9}$$

This late equation led to the previous writing of the linear transformation formalism for both 3D models (Molodensky and Bursa) in their rotation terms. In reality, the linearization lightens and facilitates the resolution by ordinary least squares (OLS) but causes a loss of precision due to concatenation to certain orders of the trigonometric functions Taylor development. One condition to recover the accuracy loss is to develop a new formalism, modify the existing one, or use high-quality data in processing (Navikova, 2020).

In this article, we are dealing with contesting, in one hand the 3D models with 2D ones like multiple regression equations (MRE's) or geodetic lines and in other hand, we confront the different resolution methods such as non-linear Levenberg–Marquardt (LM) and general linear least square (LLS).

3.1.2 Second assumption

In equation (6), the three coordinates of the barycenter should take into consideration the ponderation of every point in the system instead of taking by default the unity values; the equation above should be rewritten as follows (equation (10)):

$$\vec{X}_{0} \begin{pmatrix} X_{0} \\ Y_{0} \\ Z_{0} \end{pmatrix} = \begin{pmatrix} \frac{\sum_{i=1}^{n} P_{i} X_{i}}{P_{i}} \\ \frac{\sum_{i=1}^{n} P_{i} Y_{i}}{P_{i}} \\ \frac{\sum_{i=1}^{n} P_{i} Z_{i}}{P_{i}} \end{pmatrix}, \quad \vec{X}_{0} \begin{pmatrix} X_{0} \\ Y_{0} \\ Z_{0} \end{pmatrix} = \begin{pmatrix} \frac{\sum_{i=1}^{n} P_{i} X_{i}}{P_{i}} \\ \frac{\sum_{i=1}^{n} P_{i} Y_{i}}{P_{i}} \\ \frac{\sum_{i=1}^{n} P_{i} Z_{i}}{P_{i}} \end{pmatrix}, \quad (10)$$
System p° 1

where P_i is the weight affected at every point in both systems. The ponderation is based on the influence of every point on the system by its quadratic error precision. Thus, the transformation deal with the centered reduced coordinates of both systems in consideration and minimize the effect of orientation by rotation around the barycenters. An alternative transformation from Cartesian to geodetic coordinates is considered in this study to face different types of coordinate files to be transformed (Cartesian and geodetic curved). For this purpose, a design derivative matrix A_{3nx3} is implemented in the code source, as illustrated in equation (1) of the Appendix (Soler et al., 2012).

3.1.3 Third assumption

In case the linear models do not respond to the error-minimizing purpose of the transformation parameters, I have

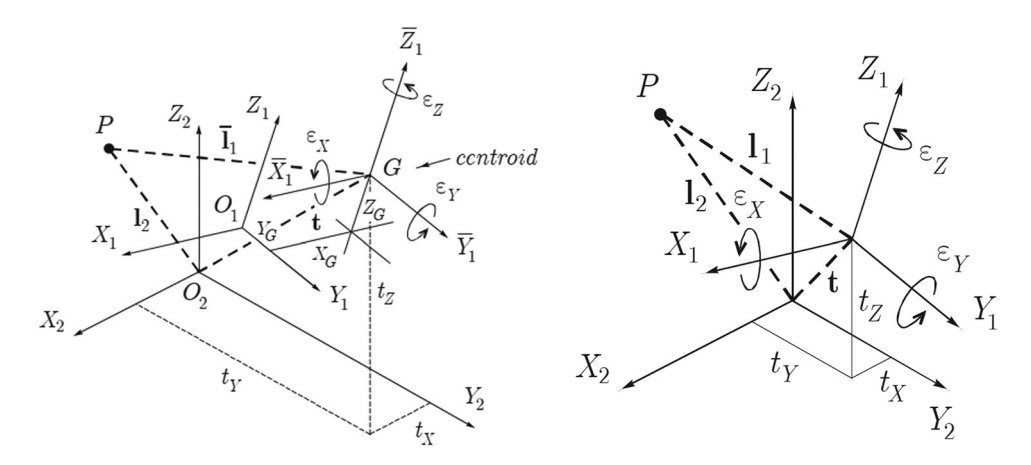


Figure 2: Illustration of Molodensky-Badekas barycenter and Bursa-Wolf transformation.

chosen the nonlinear least squares method for performing the equation system resolution adapted to our specific problem in order to avoid the accuracy loss due to truncation.

The LM is considered the most appropriate algorithm to resolve this problem efficiently because it takes into account the nonlinear aspect of formalism and is powerful to perform the resolution of nonlinear regression problems with a least squares stabilization parameter μ_k to improve the behavior of the algorithms around the minima.

Like all nonlinear optimization methods, LM is iterative. Initiated at the starting point X_0 , the method produces a series of vectors X_1 , X_2 , ... that converge toward a local minima X^+ for a regression function F described as follows:

$$F(X + \delta_X) \approx F(X) + I\delta_X,$$
 (11)

where I is the Jacobian of the function based on the first derivative of $F(\partial F/\partial X)$, hence, at each step, it is required to find δ_X that minimizes the quantity:

$$||Y - F(X + \delta_X)|| \approx ||Y - F(X) - I\delta_X||.$$
 (12)

By resolving the equation above with δ_X as a solution of nonlinear least squares, we have to bypass the embarrassing linearization passage and thus preserve the accuracy of the model.

4 Observations quality analysis in the least squares adjustment

4.1 Variance factor estimation

The variance factor (a posteriori standard deviation) is given by the following formula:

$$\hat{\sigma}_0^2 = \frac{\hat{V}^T P \hat{V}}{n - n},\tag{13}$$

where n - p is the redundancy factor (number of degrees of liberty of the problem), \hat{V} is depending directly on $\hat{\sigma}_0^2$.

Unity variance value estimation allows to provide information relevant to the observations weight matrix and residues vector (lacks in measures, errors of the model, etc.) (Collilieux et al., 2016).

4.2 Residues and normalized residues estimation

After geodetic network adjustment, the assessed solution $\hat{\chi}$ allows us to compute the observation residues as follows:

$$\hat{V} = A\hat{x} - Y. \tag{14}$$

The normalized residues u_i are computed from the following formula:

$$u_i = \frac{\hat{v}_i}{\sigma_{\hat{v}_i}}. (15)$$

In next step, the statstical analysis are shown as below:

4.2.1 Chi-squared test

The chi-squared test has the purpose of assessing a global judgment about the conformity hypothesis of residue distribution with normal distribution.

Let χ_r^2 be considered as a sum of the distribution of squares of r random normal-centered reduced variables given by the following formula:

$$\chi_r^2 = \sum_{i=1}^r \chi_i^2,$$
 (16)

with $x_i \in N(0;1)$.

The probability density of this function is

$$h_r(x) = \frac{1}{\Gamma(r/2)2^{r/2}} \times x^{\frac{r}{2}-1} \times \exp\left(-\frac{x}{2}\right) \text{ for } x \ge 0,$$
 (17)

$$h_r(x) = 0$$
 for $x < 0$,

$$\Gamma(n) = (n-1)!$$
 for $n \in N$,

and

$$\Gamma\left(n + \frac{1}{2}\right) = \Gamma\left(n + \frac{1}{2}\right) = \frac{(2n)!\sqrt{\pi}}{n!2^{2n}}.$$
 (18)

The test on zero assumption $H_0(\sigma_0^2 = \hat{\sigma}_0^2)$ is performed based on the threshold choice of probability noted α , (e.g., the value 0.05 means that the hypothesis is formulated so that it has a 95% chance of being verified). The computation of χ^2 values of χ_1^2 and χ_2^2 limits was performed using the following formulas:

$$pr(\chi_1^2 < \chi < \chi_2^2) = 1 - \alpha,$$
 (19)

$$\chi^2 = (n - p) \times \frac{\hat{\sigma}_0^2}{\sigma_0^2} = \frac{\hat{V}^T P V}{\sigma_0^2},$$
 (20)

$$\chi_1^2: \int_0^{\chi_1^2} h_{n-p}(r) dr = \frac{\alpha}{2},$$
 (21)

$$\chi_2^2: \int_0^{\chi_2^2} h_{n-p}(r) dr = 1 - \frac{\alpha}{2},$$
 (22)

where σ_0 and $\hat{\sigma}_0^2$ represent, respectively, the variance factor of a priori estimated variance.

If $\chi_1^2 < \chi^2 < \chi_2^2 \Rightarrow$ hypothesis $\sigma_0^2 = \hat{\sigma}_0^2$ is accepted (hypothesis H₀). If the zero hypothesis is accepted (hypothesis H0), thus the adjustment is considered correct. This hypothesis rejection is assimilated like an anomaly occurrence indicator (Plag, 2020). In this case, the causes are as follows:

- irrealistic observations ponderation;
- errors occurrence;
- residual systematism existence.

4.2.2 Student test

Student test is based on the determination of limits values b_1 and b_2 of tolerance interval as follows:

$$b_{1,2} = \bar{m} \pm t \cdot \sigma, \tag{23}$$

with t as the critical value of *Student* distribution, given by usual statistical tables. This value depends on redundance n-1 and probability threshold α (Akyilmaz, 2007). \bar{m} and σ denote the means and standard deviation of the residues vector, respectively. If a residues vector component does not belong to the interval $[b_1, b_2]$, the corresponding observation should be rejected.

4.2.3 Tau (τ) test

Tau test consists of verifying the conformity of normalized residues u_i to the normal law centred reducted, with risca, u_i is it belonging to the interval N (0,1).

The distribution of Tau (τ) can be derived from the distribution of student using the following formula:

$$\tau = \frac{\sqrt{Ndl} \cdot t_{ndl-1}}{\sqrt{Ndl - 1 + t_{Ndl-1}^2}},$$
 (24)

with Ndl (= n-1) as the number of degree of liberty of residues and t as the critical value of "Student" distribution.

If a component u_i of the vector of normalized residuals satisfies the inequality: $|u_i| > \tau_c$, where τ_c is the critical value of Tau following the probability threshold a, then the corresponding observation must be rejected.

5 Statistical study and results validation

For the validation purpose of this study, a set of 12 benchmarks (points whose coordinates are known in both systems) from the zero-order North Algerian network (Figure 3) are used. Indeed, the results obtained by implementing the 3D Molodensky–Badekas and Bursa–Wolf models show how much the two methods are almost similar but differ slightly in the triangular superior elements of variance–covariance matrix (VCV) (Table 2).

The two global methods lead practically to the closed results on residues except that the Molodensky-Badekas formalism gives non-correlated parameters which means that minimal variance is well reached in the case of Molodensky-Badekas than Bursa-Wolf. Indeed the reduction of benchmark coordinates according to the centroid (barycenter) ones mitigates the effect of rotation between the two systems and thus decreases the errors over the geodetic points positions (Hashemi et al., 2013) and even their root mean square (RMS) (Table 1). The VCV matrix in Tables 2 and 3 clearly indicates the difference in precision between Molodensky and Buras-Wolf as displayed in bold, higher variance values indicate less precise results. The normal character denotes less correlation over the transformation parameter errors, thus more precision in the case of Molodensky-Badekas. In order to increase the reliability of transformation parameters, another 2D formalism should be adopted and compared to the 3D ones to

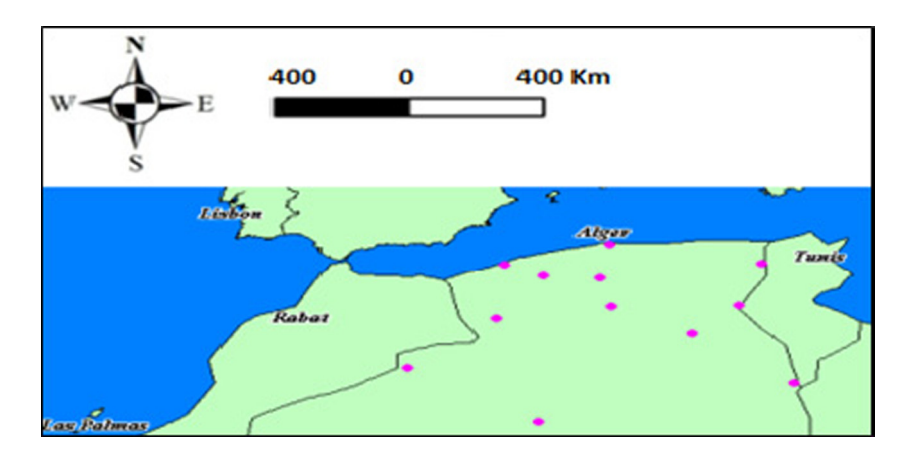


Figure 3: Distribution of zero-order North Algerian network of used benchmarks set for algorithm validation.

Table 1: Computed transformation parameters and their accuracies compared with Algerian parameters (Institut National de Cartography et de Teledetection, INCT): a case of both formalisms (MB, BW)

Parameters	Bursa-Wolf	Molodensky–Badekas	INCT official II
T_X (m)	76.0382 ± 0.0256	51.815 ± 0.01670	209.36300
T_{Y} (m)	-46.4270 ± 0.0247	-62.000 ± 0.0121	087.81700
T_{Z} (m)	-114.334 ± 0.0312	-106.000 ± 0.03070	-404.61900
δk (ppm)	1.4344 ± 0.0261	1.6340 ± 0.00216	1.4547220
\mathcal{E}_{X} (s)	-0.12494 ± 0.0660	-1.40041 ± 0.04820	-0.0046122
\mathcal{E}_{γ} (s)	-0.4534 ± 0.1067	2.50843 ± 0.1300	-3.4784221
\mathcal{E}_{Z} (s)	0.0998 ± 0.0668	-0.04657 ± 0.0500	-0.5804847

Table 2: Correlation matrices of transformation parameters obtained by two formalisms (MB and BW) with assumptions

Correlation matrix (Bursa–Wolf)								
1	-0.402	-0.242	-0.591	-0.267	-0.790	0.602		
-0.406	1	0.570	-0.236	0.785	0.290	-0.842		
-0.242	0.578	1	-0.566	-0.259	0.728	-0.098		
-0.491	-0.236	-0.566	1	-0.154	-0.817	0.576		
-0.267	0.785	-0.259	-0.154	1	0.164	-0.408		
-0.790	0.290	0.728	-0.817	0.164	1	-0.324		
0.602	-0.842	-0.098	0.576	-0.408	-0.324	1		

	Correlation matrix (Molodensky–Badekas)								
1	0.137	0.497	-0.099	-0.777	0.294	0.199			
0.137	1	0.2.76	-0.744	0.464	0.0918	-0.108			
0.497	0.276	1	-0.079	0.186	0.380	-0.430			
-0.993	-0.734	-0.079	1	0.193	-0.710	0.278			
-0.771	0.464	0.186	0.193	1	0.174	-0.415			
0.294	0.095	0.382	-0.746	0.174	1	-0.266			
0.199	-0.108	-0.433	0.278	-0.415	-0.266	1			

Bold values are the more significant.

carry out the effect of the third dimension on the accuracy of these parameters (Zavoti and Kalmár, 2016).

Among these most commonly used formalisms, we can note multiple regression MREs, affine transformation, and others. For this purpose, we have converted geographic coordinates in both systems to Cartesian ones (Ligas and Banasik, 2011).

Institute of Cartography and Remote Sensing (INCT) undertook the computation of transformation parameters over the same GNSS observation points (12 points in North of Algeria) and found the values reported in Table 1.

The global RMS of these computations, which is approximatively equal to 0.9288 m for translations and 0.143 s for rotations for all components, is considered acceptable for cartographic work. In comparison to the standard deviation of INCT transformation parameters reported in the last column of Table 1, the accuracy reached in our case seems to be satisfactory (the maximum value was 0.03 m for Bursa-Wolf in Z-translation). In the histogram of Figure 5, RMS values of the determined parameters are far less than the values of the adopted parameters (INCT) because, wherever the method is used, it does not exceed 0.25 m. The geographic transformation as "VEIS" formalism is converted to a Cartesian one by the conversion of geographic coordinates (Featherstone, 2008), (George, 1999).

In Table 2, it is well demonstrated that the number of correlation coefficient values greater than half is 19 for the Bursa Wolf (BW) model and six for the Molodensky Badekas (MB) model. It denotes that Molodensky-Badekas formalism Aström (2001), by introducing the barycenter, decreases the correlations between the double points and

Table 3: Accuracies obtained by GLS resolution for two global models without assumptions compared to MRE's

Model	Component	Minimum (m)	Maximum (m)	Mean (m)	RMS (m)
Bursa-Wolf	Χ	-1.685	2.686	1.293	1.838
	Υ	-1.221	1.164	0.697	0.834
	Ζ	-2.144	1.307	0.461	1.018
Molodensky Badekas model	Χ	-1.957	0.407	-0.941	1.014
	Υ	1.242	0.541	0.602	0.413
	Ζ	2.120	2.019	-1.398	2.058
Multiple regression equations	Λ	-0.063	0.319	0.110	0.164
	Φ	-0.407	0.634	-0.164	0.366

Table 4: Accuracies obtained by GLS resolution for two global models with assumptions compared to MRE's

Model	Component	Minimum (m)	Maximum (m)	Mean (m)	RMS (m)
Bursa-Wolf	Χ	-1.426	2.686	1.293	0.238
	Υ	-0.301	1.164	0.697	0.434
	Z	-1.491	1.307	0.461	1.018
Molodensky-Badekas model	Χ	-1.417	0.407	-0.841	0.801
	Υ	0.238	0.541	0.404	0.354
	Z	-2.033	2.019	-1.308	1.158
Multiple regression equations	Λ	-0.063	0.319	0.110	0.164
	Φ	-0.407	0.634	-0.164	0.366

thus attenuates the propagation of errors on the transformation parameters. If a point is suspect or badly defined, the reduction of its coordinates to those of the barycenter is supposed to decorrelate the errors and thus reduce their propagation.

5.1 Comparison between linear (general least square, GLS) and nonlinear adjustment (LM)

The comparison is not only limited to the use of transformation formalism but also concerns the adjustment technique used in relation to the type of problem to be resolved. Indeed, we are sometimes faced with particular cases of nonlinear systems that need special fitting techniques like "Levenberg–Marquardt," "Steepest Decent," "Newton algorithm" and many others (Ruffhead, 2020, 2021).

In this work, I have opted for LM to analyze and compare its purpose with that of the linear method "GLS" as it

occurs. As mentioned in the third assumption above, this method does not take into consideration the linearization problem and thus avoids truncation of the equation using the Taylor development until certain order and no information about the system would be lost, thus preserving the accuracy of the results shown in Tables 3 and 4. Considering the Bursa–Wolf transformation as an example, the equation can be written as follows:

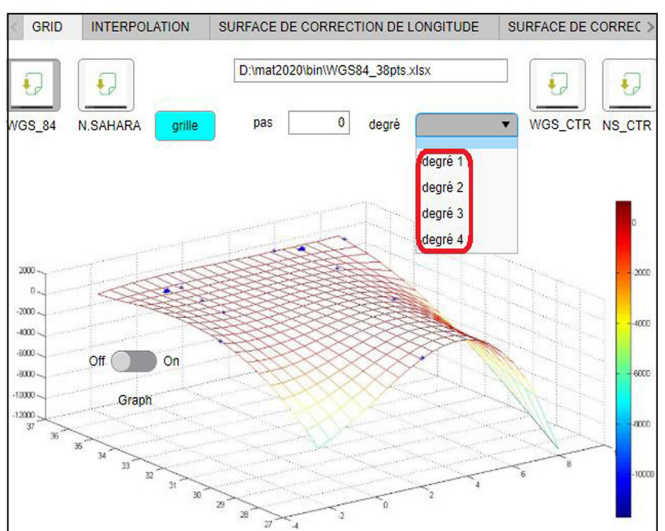
$$I_2 = (1 + ds)(I + U)I_1 + t_2,$$
 (25)

where $I_1 = \begin{bmatrix} X & Y & Z \end{bmatrix}_1^T$ and $I_2 = \begin{bmatrix} X & Y & Z \end{bmatrix}_2^T$,

ds is a very small quantity, and $t_2 = [t_X \ t_Y \ t_Z]_2^T$ is a vector of translation between the two systems (Deakin, 2006).

The above equation is considered simultaneously for a nonlinear process using the LM algorithm and a linear one illustrated by GLS. In the following, we present the comparison of results between the two fitting methods for both transformations.

The Table 4 present the results of statistical analysis for the global models and the multiple regression MRE's



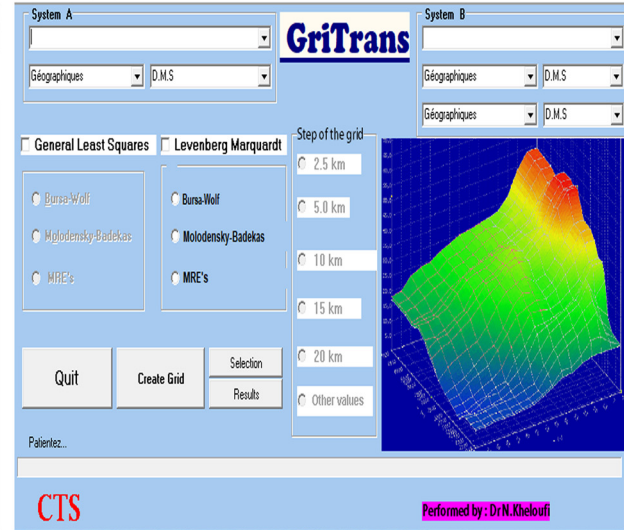


Figure 4: Screenshot of the application interface including both techniques.

algorithm. Table 3 concerns the generalized least squares, and Table 4 shows the nonlinear fitting of the global (3D) models. Globally, the RMS turn around the meters in the worst case (>2.058 for Molodensky-Badekas) and less than 20 cm for the MRE's model. This denotes the possibility of improving the precision of position in the optimum case; geodetic positioning sometimes needs sub-centimeter (geodynamics and technical auscultation) as accuracy to be satisfied. In Table 5, was reported the same models processed by LM algorithm with resolving the equation (12), δ_X is thus a solution of the nonlinear system applied for all models. For this purpose, all models and both linear and nonlinear algorithms have been implemented in the « Delphi10 » application (Figure 4). A GLS solution has been introduced to determine a unique set of geodetic coordinates, with accompanying accuracy prediction coordinates from different observing scenarios (Soler et al., 2012).

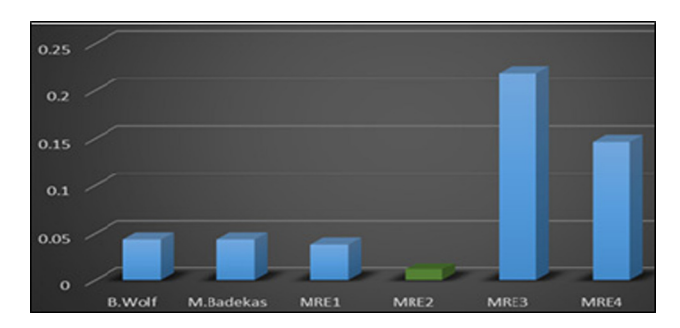


Figure 5: Variation of parameters RMS in meters for the used techniques (global models adjusted with GLS) and MREs.

According to the Table 5, the LM algorithm improves the accuracy of the global models if we take into consideration different assumptions (Acar, 2006). In this case, there is no need to appeal the multiple regression method because, for certain applications (geodetic works), we need to transform 3D cartesian components (X, Y, Z).

Nevertheless, the MRE remains interesting for limited area transformation in the case of cadastral surveys. In Figure 4, the choice of the degree of MRE is decisive for better accuracy; in our example, the choice of degree two in the interface (red framed degrees choices in Figure 4) is more suitable to obtain less error in transformation calculus (Figure 5), whereas degree three is not numerically stable because of the minus sign in the regression factors.

We could improve the quality of transformation parameters issued by GLS by Zoning fitting and considering a zonage for a wide area, *i.e.*, processing the method by set of benchmarks belonging to several restricted areas. In this case, we have partially resolved the problem because the obtained parameters are regional and not global, which is useful for a restricted area (Hok Sum, 2003).

In Tables 3–5, we present the results of data processing by both 3D and 2D models (Bursa–Wolf, Molodensky–Badekas, and MRE) with and without the assumptions explained above for carrying out the contribution of each model and also the contribution of assumptions taken into account in the improvement of precision in the processing of geodesic networks.

For the global models, it is clear from tales that the three considered assumptions have brought improvements in accuracy (Table 4) better than the improvements

Table 5: Results and analysis of the nonlinear (LM) process over the two global models

Model	Component	Minimum (m)	Maximum (m)	Mean (m)	RMS (m)
Bursa-Wolf	Χ	0.126	0.686	1.293	0.213
	Υ	-0.101	0.164	0.697	0.762
	Z	0.572	1.102	0.461	1.015
Molodensky-Badekas model	Χ	-1.223	0.311	-0.841	0.906
	Υ	0.103	0.264	0.404	0.325
	Ζ	-1.695	1.019	-1.308	1.065

Table 6: Student and chi-square test over the longitude

Sigma a priori (σ_0)	Sigma a posteriori ($\hat{\sigma}_0$)	Chi-square test	Student test
0.025 s	0.014	Positive	Zero suspect observation

The variable σ_0 denotes the a priori standard deviation, which is equal to ± 0.025 s relevant to the reference "Nord Sahara" benchmarks in the North Algeria zone (Figure 3), and $\hat{\sigma}_0$ denotes the calculated standard deviation of the residues vector.

Table 7: Student and chi-square test over the latitude

Sigma a priori (σ_0)	Sigma a posteriori ($\hat{\sigma}_0$)	Chi-square test	Student test
0.025 s	0.017	Positive	Zero suspect observation

The variable σ_0 denotes the a priori standard deviation, which is equal to ± 0.025 s relevant to the reference "Nord Sahara" benchmarks in the North Algeria zone (Figure 3), and $\hat{\sigma}_0$ denotes the calculated standard deviation of the residues vector.

brought about by the implementation of nonlinear least squares analysis "LM". Indeed, the precisions revolve around 35 cm with Molodensky–Badekas and 40 cm with Bursa–Wolf once the assumption is considered (Table 4) compared to the results of Table 3, where these hypotheses have been omitted (Yang, 2014).

The results of Tables 3 and 4 show that 2D model MRE minimizes errors, and even its statistical analysis is very good considering the tests undertaken on it.

5.2 Results of statistical analysis over MREs

For the degree of freedom (DOF) = 4, a statistical test was performed over the multiple regression method relevant to the equation 24 of paragraph 3.2. The results obtained from the Student and chi-square tests (Zeggai, 2006) are shown in Tables 6 and 7.

5.3 Over the latitude

The origin of the ITRF2020 long-term frame is defined in such a way that there are zero translation parameters at epoch 2015.0 and zero translation rates between the ITRF2020 and the international laser ranging service solar lunar ranging long-term frame over the time span 1993.0-2021.0 UNGGIM (2017), (Table 8).

Altamimi (2022) considered that ITRF 2020 is very close to WGS84 in such a way as to consider them almost confused. That lead to consider a part of WGS84 data as of good quality even the classical North Sahara coordinates are badly determined as cited in the Introduction.

6 Discussion

After considering these assumptions, we can say that we are in conformity with the directives and resolutions of the "UN-GGIM" concerning the use of the international geodetic frames and attachment of our local systems to the latest versions of ITRF to minimize position errors during compensations because the difference between the ITRF2018 and the WGS84 is some centimeters. The global 3D models processed with OLS seem to be the most used and famous for this purpose. Nevertheless, in different fields of engineering and earth science, certain cases need more accuracy; the ordinary linear least squares prove to be limited.

Thus, we have to use new numerical methods of resolution that can provide great efficiency in polynomial modelization. Therefore, instead of being limited to linear models, we have to apply the nonlinear least squares resolution to resolve the transformation problem between geodetic systems.

This need appears especially in the case of the Nord Sahara datum (Algeria), on which the linear models are not very appropriate because of the lack of information about the geoid's undulation (the third component is not accurately determined). In this article, our main aim is to carry out the importance of using the nonlinear least squares method (LM) applied over two 3D (global transformation) models and a 2D one (MRE) on a huge area benchmarks network (North Algeria).

Coordinate transformation parameters and their RMS have been computed by both the OLS and LM algorithms compared with multiple regression (Kheloufi et al., 2009) to compare, on the one hand, the linear adjustment within its two variants (local and global) with the MRE's and, on the

Table 8: Transformation parameters at epoch 2015.0 and their rates from ITRF2020 to ITRF2014 (ITRF2014 minus ITRF2020)

	<i>T</i> ₁ (mm)	T ₂ (mm)	<i>T</i> ₃ (mm)	D (10 ⁻⁹)	R ₁ (mas)	R ₂ (mas)	R ₃ (mas)
	-1.4	-0.9	1.4	-0.42	0.000	0.000	0.000
±	0.2	0.2	0.2	0.03	0.007	0.006	0.007
Rates	0.0	-0.1	0.2	0.00	0.000	0.000	0.000
±	0.2	0.2	0.2	0.03	0.007	0.006	0.007

other hand, the linear adjustment and the nonlinear one. In this context, a set of 12 benchmarks localized in North Algeria have been integrated to compute the transformation parameters (3D and 2D). Tables 3, 4, and 5 show the difference in accuracies between different models (BW, MB, and MRE's) processed by the same method (GLS) and also the difference between the methods themselves, i.e., GLS vs. LM. For example, the Molodensky formalism (Deakin, 2006) generally gave better precision when processed by GLS for the X and Y components (1.014 m against 1.838 m) except for the Y component, where Bursa-Wolf is near the meter when Molodensky-Badekas is about 2 m. Multiple regression, which is a 2D formalism, ensures submeter accuracy and is adapted for wide-area transformation processing like in North Algeria. In our case, for a near 500 km baseline length, the method turned out to be very efficient because it did not exceed a meter. For the global models, we could reach these performances with precision only because we have taken into consideration the assumptions cited above (assumptions 1, 2, and 3).

Previous studies that have been performed without including a hypothesis have given error-blemished results with less accuracy (Table 5). For both global models, we could not reach the submeter for several components, where even the *X* and *Y* components outperformed the geodetic expected errors.

The purpose of this work was to develop a solution to the crucial problem of transformations between geodetic reference frames, particularly between the system in force in Algeria, the North Sahara - Clarke 1880, and the system in which the coordinates resulting from the GPS campaigns are expressed, i.e., the WGS84. Through this multicriteria analysis, we could prove that the coordinate transformation problem could be solved to carry out reliable transformations within acceptable precisions for different applications (geodetic, geodynamic, and land survey). The calculation of these parameters required an investigation into the existence of double-point files of impeccable quality and homogeneous and dense exhaustiveness. This led us to use some files from previous undertaken by different institutions (centre des techniques spatiales, INCT, entreprise nationale de geophysique) and in different projects: PUBLIC WORKS DIVISION-DTP-Oran network, Reseau geodesique de Sonatrach-Sonatrach project, North Algeria densification campaign, etc., where the set of points are determined with a priori centimeter precision standard deviations.

As the determination of the transformation parameters is also based on the numerical models and mathematical formalisms, our work focused on the treatment of double points in our disposition by different methods:

- · 3D model of Molodensky-Badekas and Bursa-Wolf,
- 2D model of multiple regression equations,
- Nonlinear LM algorithm confronted with LLS.

The results presented in this study highlight the strengths and weaknesses of each model on the basis of the parameter standard deviation and even the position RMS, as well as the residuals after transformations, as illustrated in tables and figures. Indeed, according to the obtained results, the comparison between the 3D models gives an advantage for the Molodensky–Badekas formalism compared to the Bursa–Wolf formalism and the advantage for the nonlinear adjustment at the expense of the linear one. The analysis made on the estimated parameters also shows a difference in precision between the 3D models and the multiple regression method, which gave low RMS (as shown in Figure 5, 2 cm for MREs and 4.5 cm for Bursa–Wolf).

As a perspective, we recommend the use of planimetric grid method with interpolation methods (plus proche voisin, bilinear, and kriging) for more accuracy improvement.

Conflict of interest: Authors state no conflict of interest.

References

Acar, M. 2006. "Deformation analysis with total least squares." *Natural Hazards and Earth System Sciences* 6, 663–669.

Akyilmaz, O. 2007. "Total least squares solution of coordinate transformation." Survey Review 39(303), 68–80.

Altamimi, Z. 2022 ITRF2020 [Data set]. IERS ITRS Center Hosted by IGN and IPGP. doi: 10.18715/IPGP.2023.LDVIOBNL.

Aström, H. 2001. Valeurs de précision lors de transformation. Office du cadastre de Berne, transformations.doc2.

Badekas J. 1969, 'Investigations related to the establishment of a world geodetic system', Report No. 124, Department of Geodetic Science, Ohio State.

Boateng, K. 2016. "Accuracy assessment of Cartesian (X, Y, Z) to geodetic coordinates (ϕ , λ , h) transformation procedures in precise 3D coordinate transformation – A case study of Ghana geodetic reference network." *Journal of Geosciences and Geomatics* 4(1), 1–7.

Bursa, M. 1962. "The theory for the determination of the non-parallelism of the minor axis of the reference ellipsoid and the inertial polar axis of the Earth, and the planes of the initial astronomic and geodetic meridians from the observation of artificial Earth satellites." Studia Geophysica et Geodetica 6, 209–214.

Collier, P. 2020. Practical Notes on Coordinate Transformation. March 2020 Swift Navigation, Inc.

Collilieux, X., Z. Altamimi, P. Rebischung, and L. Métivier. 2016. "ITRF2014: A new release of the International Terrestrial Reference Frame modeling nonlinear station motions." Journal of Geophysical Research: Solid Earth.

¹ "United Nations Committee of Experts on Global Geospatial Information Management for Arab States"

- Deakin, R. E. 2006. "A note on the Bursa-Wolf and Molodensky-Badekas transformations." School of Mathematical & Geospatial Sciences RMIT University.
- Featherstone, W. E. 2008. "Closed-form transformation between geodetic and ellipsoidal coordinates." Western Australian Centre for Geodesy & The Institute for Geoscience Research, Curtin University of Technology, GPO Box U1987, Perth, WA 6845, Australia.
- George, P. 1999. "Transforming Cartesian coordinates X,Y,Z to geographical coordinates φ, λ, h." *Department of Land Information Royal Melbourne Institute of Technology GPO Box 2476V, MELBOURNE, VIC, 3001, Australian Surveyor* 44(1), 55–63.
- Hashemi, A, M. Kalantari, and M. Kasser. 2013. "Direct solution of the 7 parameters transformation problem." *Applied Mathematics & Information Sciences* 7(4), 1375–1382.
- Helmert, F. R. 1907. Die Ausgleichungsrechnung de der Methode der Square: mit Anwendungen auf die Geodäsie und die Theorie der Messinstrumente, Teubner Verlag, Leipzig 1907.
- Hok Sum, F A. 2003. "Comparative analysis of the performance of iterative and non-iterative solutions to the Cartesian to geodetic coordinate transformation." *Journal of Geospatial Engineering* 5(2), 61–74.
- Kheloufi, N, S. Kahlouche, and R. Lamara. 2009. "Nonlinear Least Squares (Levenberg–Marquardt algorithms) for geodetic adjustment and coordinates transformation." *Geophysical Research Abstracts*, Vol. 11, EGU-2009-333, 2009 EGU General Assembly 2009.
- Kheloufi, N. 2012. "Coordinates transformation by 'Zoning Method' for parameters computing between WGS84 and North Sahara." Proceeding of the European Geosciences Union (EGU) Vienna 2012.
- Ligas, M. and P. Banasik. 2011. "Conversion between Cartesian and geodetic coordinates on a rotational ellipsoid by solving a system of nonlinear equations." *Geodesy and Cartography, Polish Academy of Sciences* 60(2), 145–159.
- Molodenskiy, M. S. 1960. Metody izucheniya vnesnego gravitatsiononogo polya i figuri Zemli. Trudy CNIIGAIK Moscow, Vyp.131.
- Novikova, E. 2020. "The change of coordinate system versus the area of parcels." *Geodesy and Cartography* 46(1), 26–33. doi: 10.3846/gac. 2020.6979.

- Plag, H. P. 2020. "Comprehensive overview of geodesy's contribution to science and society." Global Geodetic Observing System Meeting the Requirements of a Global Society on a Changing Planet.
- Ruffhead, A. 2020. Introduction to geodetic datum transformations and their reversibility. March 2020 In book: UEL ACE Surveying Working Paper No 01/2020.
- Ruffhead, A. 2021. "Derivation of rigorously-conformal 7-parameter 3D geodetic datum transformations." *Survey Review* 53(376). doi: 10. 1080/00396265.2019.1665614.
- Soler, T, J. Y. Han, and N. D. Weston. 2012. "Alternative transformation from Cartesian to geodetic coordinates by least squares for GPS georeferencing applications." *Mathematics & Computer Science*, *Geosciences*. doi: 10.1016/j.caqeo.20110.026.
- United Nations Global Geospatial Information Management (UN-GGIM). 2017. Report to 7th Session about the UN-GGIM Arab States Activities.
- Wolf, H. 1963. "Geometric connection and re-orientation of threedimensional triangulation nets." *Bulletin Grodesique* 68, 165–169. doi: 10.1007/BF02526150.
- Yang, C. S. 2014. "Development of the process of coordinate transformation of local datum cadastral map to the world geodetic system-using adjusted coordinates." Journal of the Korean Society of Surveying Geodesy Photogrammetry and Cartography 32(spc4_2), 401–412. doi: 10.7848/ksgpc.2014.32.4-2.401.
- Zavoti, J. and J. Kalmár. 2016. "A comparison of different solutions of the Bursa–Wolf model and of the 3D, 7-parameter datum transformation." *Acta Geodaetica et Geophysica* 51, 245–256.
- Zeggai, A. 2006. Application de l'approchepar les équations de la régressionmultiple pour le passage d'undatum à l'autre (cas de l'Algérie), Revue XYZ N° 106 1er trimestre 2006.
- Ziggah, Y., H. Youjian, P. B. Laari, and Z. Hui. 2017. "Novel approach to improve geocentric translation model performance using artificial neural network technology." *BCG-Boletim de Ciências Geodésicas On-Line version*. doi: 10.1590/S1982-1702017000100014.

Appendix

A1 Mathematical formulation of coordinates conversion

The basic mathematical relationship between Cartesian and orthogonal curvilinear geodetic coordinates is attributed to Helmert and can be written in matrix form as follows:

$$\begin{bmatrix} x \\ y \\ z \end{bmatrix} = \begin{bmatrix} (N+h)\cos\phi\cos\lambda \\ (N+h)\cos\phi\sin\lambda \\ (N(1-e^2)+h)\sin\phi \end{bmatrix},$$
 (A1)

where $N=\frac{a}{W}$ is the principal radius of curvature along the prime vertical and $M=\frac{a(1-e^2)}{W^3}$ is the principal radius of curvature along the meridian with $W^2 = 1 - e^2 \sin^2 \phi$ and $e^2 = 2f - f^2$.

In all the above equations, a and f are the semi-major axis and flattening of the selected ellipsoid, respectively.

A2 Least squares methodology for coordinates conversion

For the least squares resolution purpose, a derivative design matrix A called Jacobian is used.

The numerical value of matrix A is determined using any initial approximation of the parameters $X_0 = \begin{bmatrix} \lambda_0 & \phi_0 & h_0 \end{bmatrix}^T$.

$$A_{3nx3} = \frac{\partial f}{\partial X} \Big|_{X_0, I_b} = \begin{bmatrix} \frac{\partial f_1}{\partial \lambda} & \frac{\partial f_1}{\partial \phi} & \frac{\partial f_1}{\partial h} \\ \frac{\partial f_2}{\partial \lambda} & \frac{\partial f_2}{\partial \phi} & \frac{\partial f_2}{\partial h} \\ \frac{\partial f_3}{\partial \lambda} & \frac{\partial f_3}{\partial \phi} & \frac{\partial f_3}{\partial h} \\ \frac{\partial f_4}{\partial \lambda} & \frac{\partial f_4}{\partial \phi} & \frac{\partial f_4}{\partial h} \\ \frac{\partial f_5}{\partial \lambda} & \frac{\partial f_5}{\partial \phi} & \frac{\partial f_5}{\partial h} \\ \frac{\partial f_6}{\partial \lambda} & \frac{\partial f_6}{\partial \phi} & \frac{\partial f_6}{\partial h} \\ \frac{\partial f_{r-2}}{\partial \lambda} & \frac{\partial f_{r-2}}{\partial \phi} & \frac{\partial f_{r-2}}{\partial h} \\ \frac{\partial f_{r-1}}{\partial \lambda} & \frac{\partial f_{r-1}}{\partial \phi} & \frac{\partial f_{r-1}}{\partial h} \\ \frac{\partial f_r}{\partial \lambda} & \frac{\partial f_r}{\partial \phi} & \frac{\partial f_r}{\partial h} \end{bmatrix}.$$
 (A2)